THE JOURNAL OF BIOLOGICAL CHEMISTRY VOL. 283, NO. 19, pp. 13320–13329, May 9, 2008


# The $CB_2$ Cannabinoid Receptor Controls Myeloid Progenitor Trafficking

## *INVOLVEMENT IN THE PATHOGENESIS OF AN ANIMAL MODEL OF MULTIPLE SCLEROSIS*[*] [S]

Received for publication, September 24, 2007, and in revised form, February 11, 2008 Published, JBC Papers in Press, March 11, 2008, DOI 10.1074/jbc.M707960200

**Javier Palazuelos[‡1], Nathalie Davoust[§2], Boris Julien[‡3], Eric Hatterer[§], Tania Aguado[‡4], Raphael Mechoulam[¶], Cristina Benito[‖], Julian Romero[‖], Augusto Silva[**], Manuel Guzmán[‡], Serge Nataf[§5], and Ismael Galve-Roperh[‡5,6]**

*From the [‡]Department of Biochemistry and Molecular Biology I, School of Biology, and Centro de Investigación Biomédica en Red sobre Enfermedades Neurodegenerativas (CIBERNED), Complutense University, 28040 Madrid, Spain, the [§]INSERM U433, Institut Féderatif Recherche (IFR) des Neurosciences de Lyon, Faculté de Médecine Laënnec, 69372 Lyon, France, the [¶]Department of Medicinal Chemistry and Natural Products, School of Pharmacy, The Hebrew University, 91120 Jerusalem, Israel, the [‖]Laboratorio de Apoyo a la Investigación, Fundación Hospital Alcorcón, 28922 Madrid, Spain, and the **Centro de Investigaciones Biológicas (CIB-CSIC), Ramiro de Maeztu 9, 28040 Madrid ,Spain*

**Cannabinoids are potential agents for the development of therapeutic strategies against multiple sclerosis. Here we analyzed the role of the peripheral $CB_2$ cannabinoid receptor in the control of myeloid progenitor cell trafficking toward the inflamed spinal cord and their contribution to microglial activation in an animal model of multiple sclerosis (experimental autoimmune encephalomyelitis, EAE). $CB_2$ receptor knock-out mice showed an exacerbated clinical score of the disease when compared with their wild-type littermates, and this occurred in concert with extended axonal loss, T-lymphocyte ($CD4^+$) infiltration, and microglial ($CD11b^+$) activation. Immature bone marrow-derived $CD34^+$ myeloid progenitor cells, which play a role in neuroinflammatory pathologies, were shown to express $CB_2$ receptors and to be abundantly recruited toward the spinal cords of $CB_2$ knock-out EAE mice. Bone marrow-derived cell transfer experiments further evidenced the increased contribution of these cells to microglial replenishment in the spinal cords of $CB_2$-deficient animals. In line with these observations, selective pharmacological $CB_2$ activation markedly reduced EAE symptoms, axonal loss, and microglial activation. $CB_2$ receptor manipulation altered the expression pattern of different chemokines (CCL2, CCL3, CCL5) and their receptors (CCR1, CCR2), thus providing a mechanistic explanation for its role in myeloid progenitor recruitment during neuroinflammation. These findings demonstrate the protective role of $CB_2$ receptors in EAE pathology; provide evidence for a new site of $CB_2$ receptor action, namely the targeting of myeloid progenitor trafficking and its contribution to microglial activation; and support the potential use of non-psychoactive $CB_2$ agonists in therapeutic strategies for multiple sclerosis and other neuroinflammatory disorders.**

During the last years, it has been shown that the endocannabinoid (eCB)[7] system, the endogenous system targeted by active ingredients of the hemp plant *Cannabis sativa L* (1), is altered in experimental autoimmune encephalomyelitis (EAE), an animal model of multiple sclerosis (MS) (2–4). In addition, cannabinoid receptor agonist administration or modulation of the eCB tone with eCB reuptake/degradation inhibitors improves pathological signs of the disease, notably spasticity and tremor (3–7). Moreover, cannabinoids have been shown to be effective not only in palliating EAE symptoms but also as neuroprotective agents that, by promoting oligodendrocyte survival (8), reducing demyelinated lesions (9), and attenuating neuronal loss (10, 11), contribute to delayed progression of the disease. This protective role of the eCB system during neuroinflammation is exerted, at least in part, by decreasing immune cell activation and infiltration (12, 13).

Cannabinoid actions are mediated by the activation of two different G-protein-coupled receptors, namely $CB_1$ and $CB_2$ receptors (1). Alleviation of EAE symptoms by cannabinoid intervention is mostly attributed to the engagement of neuronal $CB_1$ receptors (4, 14), whereas $CB_2$ receptor expression by infiltrating T-cells and monocytes is involved in the control of neuroinflammation (4). Likewise, $CB_2$ receptors are functional in microglial cells, in which they inhibit the production of proinflammatory cytokines and oxygen and nitrogen reactive species (12, 15), and their expression is up-regulated upon cell activation (16). The involvement of microglial cell activation in the

* This work was supported by grants from the Picasso Program (Grant HF2005-0017), Comunidad Autónoma de Madrid (Grants S-SAL/0261/2006 and 950344), Santander Complutense (Grant PR27/05-13988), Fundación de Investigación Médica Mutua Madrileña Automovilística, Ministerio de Educacion y Ciencia (Grants SAF2004/00237), the French Embassy in Spain, and Association pour la Recherche sur la Sclerose en Plaques. The costs of publication of this article were defrayed in part by the payment of page charges. This article must therefore be hereby marked "*advertisement*" in accordance with 18 U.S.C. Section 1734 solely to indicate this fact.

[S] The on-line version of this article (available at http://www.jbc.org) contains a supplemental table.

[1] Supported by the Ministerio de Educación y Ciencia (Formación de Personal Investigador program; Spain).

[2] Present address: INSERM U851, Universite de Lyon, 69365 Lyon Cedex 07, France.

[3] Supported by the Fondation pour Recherche Medicale (France).
[4] Supported by the Comunidad Autónoma de Madrid (Spain).

[5] Both authors contributed equally to this work.

[6] To whom correspondence should be addressed. Tel.: 34-913944668; Fax: 34-913944672; E-mail: igr@quim.ucm.es.

[7] The abbreviations used are: eCB, endocannabinoid; EAE, experimental autoimmune encephalomyelitis; MS, multiple sclerosis; PBS, phosphate-buffered saline; GFP, green fluorescent protein; EGFP, enhanced GFP; WT, wild-type; PBMC, peripheral blood mononuclear cell; FAAH, fatty acid amide hydrolase; MAGL, monoacylglycerol lipase.

evolution and progression of different neurological disorders (MS, stroke, Alzheimer disease, amyotrophic lateral sclerosis, human immunodeficiency virus-associated dementia) has been put forward (17, 18),[8] and it is becoming evident that, besides central nervous system-resident microglial cells, bone marrow-derived cells infiltrate the inflamed central nervous system and differentiate into functional microglia (19–21). Among those cells, $CD34^+$ myeloid progenitors expand in the blood of EAE mice, target the inflamed central nervous system, and display differentiation potential toward microglia (22). As modulation of cannabinoid signaling may result in unwanted psychoactive actions mediated by neuronal $CB_1$ receptors, the use of $CB_2$-selective agonists is an attractive therapeutic possibility (15, 23). The present study was therefore aimed at elucidating the role and action mechanism of the $CB_2$ cannabinoid receptor in EAE. In particular, we focused on the trafficking of myeloid progenitors toward the inflamed spinal cord and their contribution to microglial activation during EAE pathogenesis.

## EXPERIMENTAL PROCEDURES

*Materials*—The following materials were kindly donated: $CB_2$ receptor knock-out mice by Nancy Buckley (National Institutes of Health, Bethesda, MD) and HU-308 by Pharmos (Rehovot, Israel). The following antibodies were used: polyclonal anti-200-kDa neurofilament heavy protein and anti-human CD11b (clone M1/70) from AbCam (Cambridge, UK); monoclonal rat anti-mouse CD45R/B220 (clone RA3–6B2) fluorescein isothiocyanate-conjugated antibody, rat anti-mouse CD11b (clone M1/70), and anti-CD4 from BD Biosciences; monoclonal anti-mouse CD34-biotin (clone RAM34) from eBioscience (San Diego, CA); polyclonal anti-$CB_2$ receptor from Affinity BioReagents (Golden, CO); monoclonal anti-human CD45RB (clone PD7/26) from Dako (Glostrup, Denmark); polyclonal anti-GFP from Invitrogen; and rabbit monoclonal anti-Ki-67 (SP6) from LabVision (Fremont, CA). Macrophage-colony stimulating factor and Flt-3 were from PreproTech Inc. (London, UK).

*Animal Procedures and EAE Induction*—Animal procedures were performed according to the European Union guidelines (86/609/EU) for the use of laboratory animals. Adult $CB_2$ receptor-deficient mice (8 weeks old) (24) and their respective wild-type littermates, housed in a temperature-controlled room with a fixed 12-h light/12-h dark cycle, were obtained from heterozygote crosses. For EAE induction, mice were immunized at days 0 and 7 by subcutaneous injection of 150 $\mu$g of myelin oligodendrocyte glycoprotein 35–55 peptide emulsified in complete Freund's adjuvant, as described previously (25). In addition, at days 0 and 2, mice were administered intraperitoneally with 500 ng of pertussis toxin (Sigma). Clinical scores were monitored using the following scale: 0, lack of clinical signs; 1, tail weakness; 2, hind limb paraparesis, hemiparesis, or ataxia; 3, hind limb paralysis or hemiparalysis; 4, complete paralysis; 5, moribund; 6, death. In pharmacological experiments, HU-308 (15 mg/kg) was administered intraperitoneally starting at the day of maximal score and thereafter daily until sacrifice. Control animals received the corresponding vehicle injections (100 $\mu$l of phosphate-buffered saline (PBS) supplemented with 0.5 mg/ml defatted bovine serum albumin and 4% dimethyl sulfoxide). Each clinical score value was obtained from a representative experiment of four or three independent experiments aimed at elucidating the effect of $CB_2$ receptor genetic ablation or HU-308 administration, respectively. Cell transfer experiments were performed by intracardiac injection of $5 \times 10^6$ bone marrow cells derived from healthy C57BL/6 (ACT$\beta$-EGFP) mice into EAE-induced wild-type (WT) and $CB_2^{-/-}$ syngenic mice at day 9 before symptom appearance. Recipient mice were sacrificed and analyzed 10 days after engraftment.

Magnetic resonance imaging was performed in EAE mice ($n = 4$ each group) the day before sacrifice at the Nuclear Magnetic Resonance Center of Complutense University (Madrid, Spain). Anesthetized mice were placed in a Biospec 47/40 (Bruker, Ettlingen, Germany) operating at 4.7 teslas, equipped with a 12-cm gradient set and using a 4-cm radio frequency surface coil. Three-dimensional T2-weighted spin-echo images were acquired using a fast spin-echo sequence. The acquisition parameters were: time recovery = 2226 ms, effective time echo = 117 ms, field of view = $2.5 \times 1.6 \times 1.0$ $cm^3$, and two averages. The acquisition matrix size was $256 \times 128 \times 32$, which was zero-filled to get a reconstructed matrix size of $256 \times 256 \times 32$. The total acquisition time was 19 min. Diffusion water images delineated the area of neuroinflammation evidenced as hyperintense signals.

*Immunofluorescence and Confocal Microscopy*—EAE mice were sacrificed, and isolated spinal cords were frozen on dry ice. Immunofluorescence analysis (26) was performed on ethanol-fixed 14-$\mu$m-thick cryostat sections. Spinal cord sections were rinsed and blocked for 30 min in PBS supplemented with 10% goat serum and 4% bovine serum albumin and, after washing, incubated with the indicated primary antibodies. Secondary antibody incubation (1 h at room temperature) was performed with the appropriate mouse, rat, and rabbit highly cross-adsorbed Alexa Fluor 488, Alexa Fluor 594, Alexa Fluor 647 secondary antibodies or with Alexa Fluor 488 or Alexa Fluor 594 streptavidin conjugates (Invitrogen). Washed sections were incubated with Hoechst 33342 (5 $\mu$g/ml) in PBS prior to mounting.

The specificity of $CB_2$ receptor immunoreactivity was corroborated by using $CB_2^{-/-}$ mouse sections, in which no immunoreactivity was observed, and allowed to adjust optimal confocal microscope settings. $CB_2$ receptor expression was analyzed with anti-$CB_2$ receptor antibody together with anti-CD11b and anti-CD34-biotinilated antibodies (overnight incubation at 4 °C) followed by secondary staining for rabbit and mouse IgGs with highly cross-adsorbed Alexa Fluor 647, Alexa Fluor 594, and streptavidin-Alexa Fluor 488 secondary antibodies, respectively. In addition, triple immunostaining was performed with a combination of anti-CD34, CD45R/B220, and $CB_2$ primary antibodies and their appropriate secondary fluorescent antibodies. All immunofluorescence data were obtained in a blinded manner by two independent observers in a minimum of 5–7 adjacent slices of two different samples from the lumbo-thoracic spinal cord of the same animal. To determine the loss of axonal surface and the extent of microglial

[8] N. Davoust, C. Vuaillat, G. Androdias, and S. Nataf, manuscript in preparation.

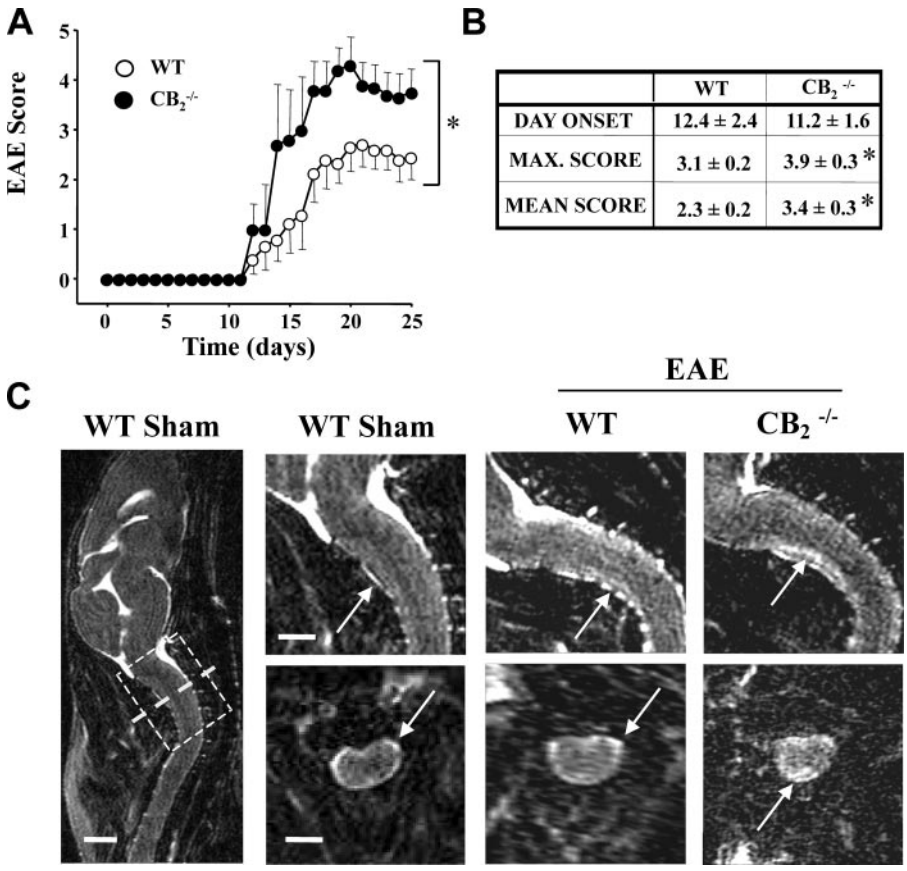


| | WT | $CB_2^{-/-}$ |
|---|---|---|
| DAY ONSET | 12.4 ± 2.4 | 11.2 ± 1.6 |
| MAX. SCORE | 3.1 ± 0.2 | 3.9 ± 0.3 * |
| MEAN SCORE | 2.3 ± 0.2 | 3.4 ± 0.3 * |

FIGURE 1. **EAE is exacerbated in $CB_2$-deficient mice.** *A*, EAE score was determined daily after induction of the disease in WT (*open circles*) and $CB_2^{-/-}$ littermates (*closed circles*; $n = 8$ each group). Scores were compared between the two groups day by day. *, $p < 0.05$ *versus* WT from day 17 on. *B*, the mean values of the day of clinical onset, maximum score, and mean score from symptom appearance are shown. *, $p < 0.05$ *versus* WT. *C*, representative MRI images at day 24 of spinal cords from WT and $CB_2^{-/-}$ mice after EAE induction are shown. The bright signal of low water diffusion areas corresponds to inflamed tissue. *Scale bars*: general axial projection (*left panel*), 2.0 mm; magnified axial projections (*top panels*), 1.3 mm; and magnified sagital projections (*bottom panels*), 1.7 mm.

activation, neurofilament H and CD11b staining was quantified with Metamorph-Offline software (Universal Imaging, Downingtown, PA) and referred to the total white matter area of spinal cord sections. T-cells, $CD34^+$ cells, and bone marrow GFP infiltration were quantified by immunoreactive positive cell counting, and results are given as mean cell number per $mm^2$. CD34 and CD31 double immunostaining was routinely performed to confirm that CD34 immunoreactivity included, in addition to $CD31^+$ vascular endothelial cells, cells with microglial features. Only $CD34^+$ cells displaying a rounded morphology (similar to ameboid microglia) or extending short processes (similar to reactive microglia) were counted. Both perivascular and parenchymal $CD34^+$ cells were observed, and a significant fraction of those cells did not express the endothelial marker CD31 and co-expressed the microglial marker CD11b. Results are given as mean cell number per $mm^2$. *In vitro* immunofluorescence was performed with the indicated primary antibodies and the corresponding secondary fluorescent antibodies (as above). Immunofluorescence controls were routinely performed with incubations in which primary antibodies were not included.

Immunofluorescence images shown in Figs. 2 and 3 were obtained with a fluorescence microscope (Zeiss Axioplan II) and acquired with a CDD camera (F-View II; Soft Imaging System). Images in Figs. 4–6 and 9 were examined using Leica TCS-SP2 software (Wetzlar, Germany) and SP2 microscope with two passes by Kalman filter and a 1024 × 1024 collection box.

*Cell Culture and Flow Cytometry Analysis*—Bone marrow cells were cultured as described (22, 27) with slight modifications. Briefly, 8-week-old female mice were sacrificed, and bone marrows were harvested by flushing out tibiae and femurs and culturing in Iscove's modified Dulbecco's medium supplemented with 4% N2 (Invitrogen), 15 ng/ml Flt-3, and macrophage colony-stimulating factor and penicillin and streptomycin. Six days after plating, non-adherent cells were harvested and, after washing, characterized by flow cytometry or replated for the generation of microglial-like cells. Myeloid progenitors were differentiated for 5 days in bone marrow culture medium (described above) supplemented with 1 volume (50%) of glial cell conditioned medium. Prior or after differentiation, adherent cells were fixed for immunofluorescence, frozen for RNA extraction, or detached for fluorescence-activated cell sorter analysis.

Peripheral blood mononuclear cells (PBMCs) were isolated by density gradient centrifugation on Ficoll (Histopaque 1077; Sigma) from blood samples obtained from the cave vein. Cells were washed with PBS and resuspended in PBS supplemented with 2% goat calf serum for flow cytometry analysis or frozen for RNA analysis. Flow cytometry was performed with $0.5 \times 10^6$ cells per condition fixed in 1% paraformaldehyde at 4 °C. Antibodies and their corresponding controls were incubated for 30 min at 4 °C in 2% goat serum-PBS and, after washing, samples were subjected to secondary antibody incubation. Ten thousand cells per recording were analyzed using a FACSCalibur flow cytometer.

*mRNA Detection and Quantification*—RNA was obtained with the RNeasy Protect kit (Qiagen, Valencia, CA) using the RNase-free DNase kit. cDNA was subsequently obtained using the SuperScript first-strand cDNA synthesis kit (Roche Applied Science, Welwyn Garden City, UK) and amplified with the primers indicated in supplemental Table 1A. $CB_1$ and $CB_2$ PCR amplifications were performed using the following conditions: 93 °C for 1 min, two rounds (30 s at 59 °C, 1 min at 72 °C, and 30 s at 93 °C), two rounds (30 s at 57 °C, 1 min at 72 °C, and 30 s at 93 °C), and 35 cycles (30 s at 55 °C, 1 min at 72 °C, and 30 s at

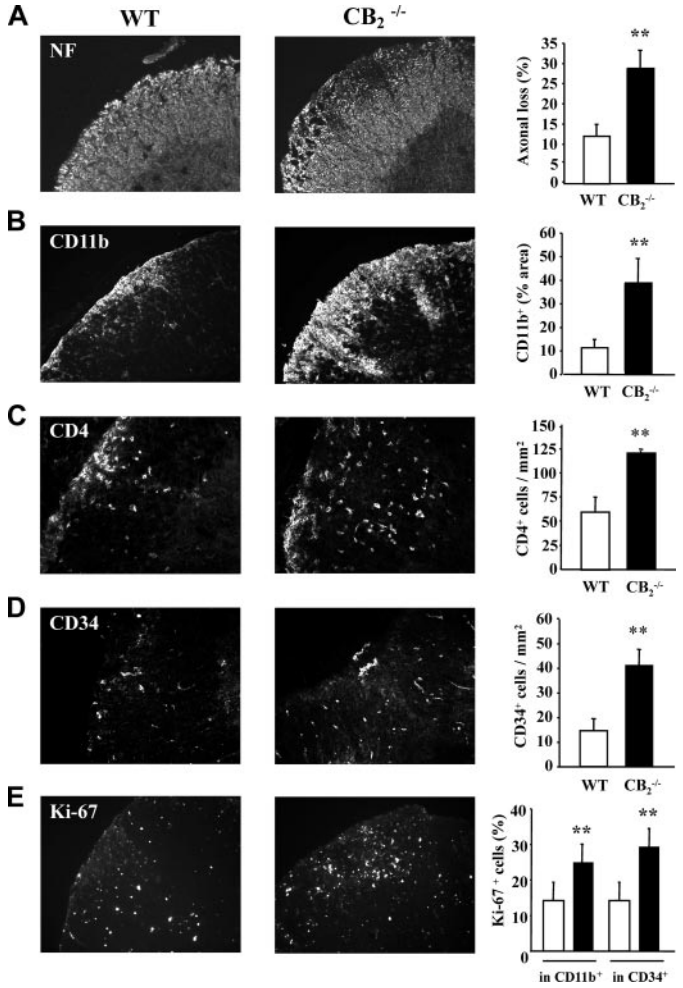


FIGURE 2. **Characterization of spinal cord sections in $CB_2$-deficient mice during EAE.** *A*, axonal loss was quantified (*right panel*) by neurofilament (*NF*) immunoreactivity in the white matter of spinal cord sections of WT and $CB_2^{-/-}$ mice at the end of the experiment. Representative immunofluorescence images are shown (*left panels*). Phenotypic analysis of infiltrating cells in spinal cord sections was performed. *B*, quantification of microglial activation was determined as the $CD11b^+$ area referred to the total area examined. *C* and *D*, the number of infiltrating $CD4^+$ (*C*) and $CD34^+$ (*D*) cells were also determined and expressed as the mean cell number per $mm^2$. *E*, proliferating cells were determined by double immunofluorescence with antibodies against *Ki*-67 and CD11b or CD34. *Scale bar*, 100 $\mu$m. **, $p < 0.01$ *versus* control.

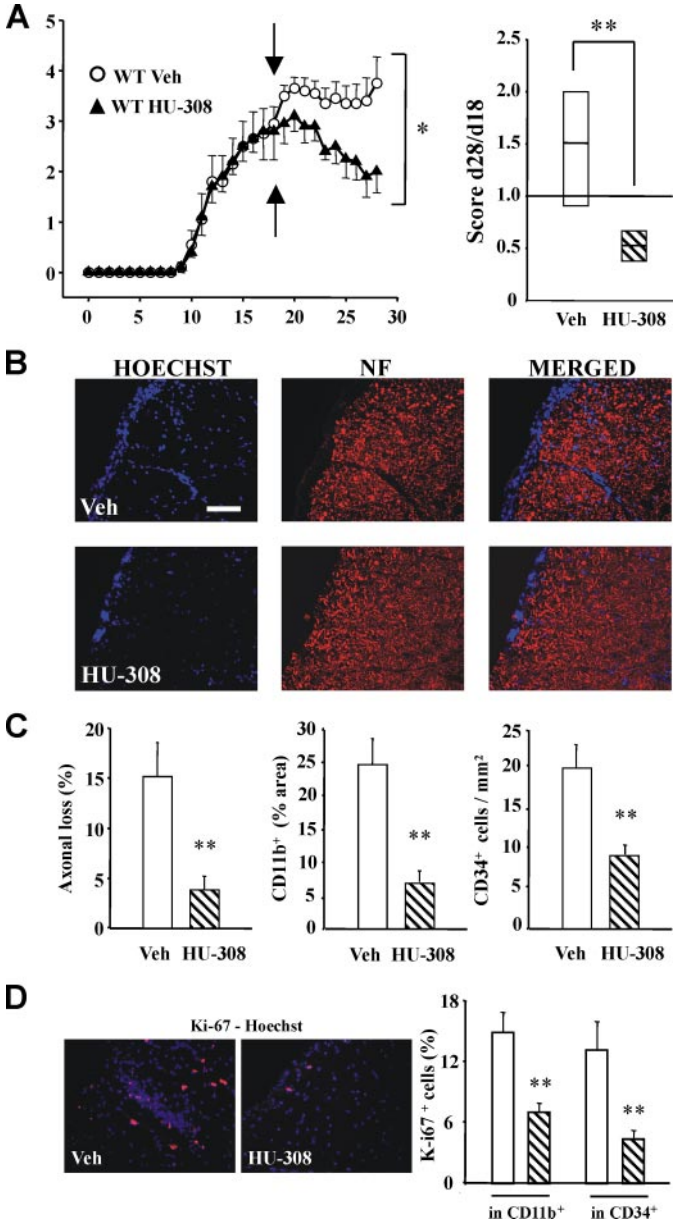


FIGURE 3. **Administration of the $CB_2$-selective agonist HU-308 improves EAE symptoms and reduces spinal cord lesions and microglial activation.** *A*, EAE score in WT mice treated with vehicle (*Veh*; *open circles*) or HU-308 (*closed triangles*; 15 mg/kg daily; $n = 5$ each group) at the indicated time point (*arrow*). *, $p < 0.05$ *versus* vehicle from day 24 on. The ratio of EAE score at day 28 to EAE score at day 18 is shown in the *right panel*. **, $p < 0.01$ *versus* vehicle. *B*, representative immunofluorescence images of neurofilament (*NF*) (*red*) and Hoechst 33342 nuclear infiltrates (*blue*) in vehicle- and HU-308-treated mice. *Scale bar*, 100 $\mu$m. *C*, quantification of axonal loss (NF immunoreactivity), microglial activation (CD11b), and CD34-positive cell infiltration. *D*, proliferating cells were determined by double immunofluorescence with antibodies against Ki-67 and CD11b or CD34. **, $p < 0.01$ *versus* vehicle.

93 °C). Finally, after a final extension step at 72 °C for 5 min, PCR products were separated on 1.5% agarose gels. Real-time quantitative PCR was performed with Universal probe system (Roche Applied Science, Basel, Switzerland) using the primers indicated in supplemental Table 1B. Amplifications were run in a 7900-HT Fast Real-time PCR system, and obtained values were adjusted using 18 S RNA levels as reference.

*Multiple Sclerosis Human Tissue Samples*—Tissue samples were supplied by the UK Multiple Sclerosis Tissue Bank, funded by the Multiple Sclerosis Society of Great Britain and Northern Ireland, Registered Charity 207495. Cortical brain samples fixed in formalin, embedded, and cut in 4-$\mu$m-thick sections were employed for immunohistochemical study as described previously (28). Briefly, sections were deparaffinized and, after washing, subjected to antigen retrieval procedure. Tissue samples were incubated with mouse anti-human CD45RB and rat anti-human CD11b monoclonal antibodies together with rabbit polyclonal anti-$CB_2$ receptor antibody.

*Statistical Analysis*—Results shown represent the means ± S.E. of the number of experiments indicated in every case. Statistical analysis was performed by analysis of variance. A *post hoc* analysis was made by the Student-Neuman-Keuls test. *In vivo* data were analyzed by an unpaired Student's *t* test.

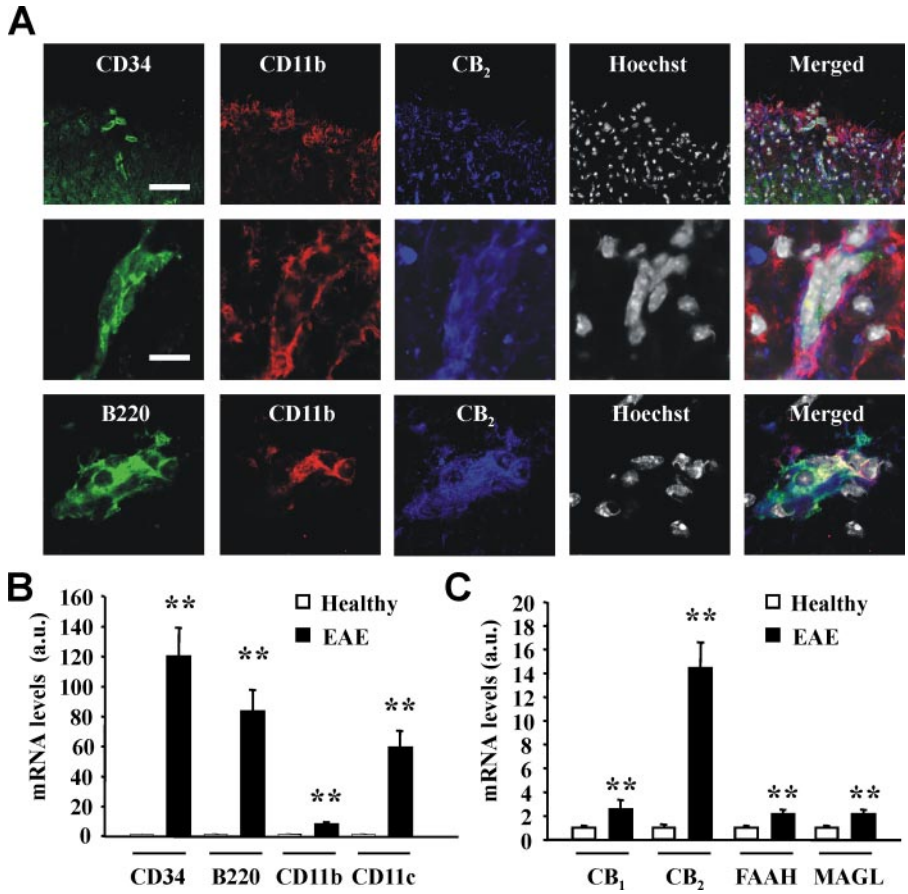


FIGURE 4. **Expression of the $CB_2$ cannabinoid receptor in spinal cord myeloid-derived microglial cells.** *A*, confocal microscopy images of EAE spinal cord sections were obtained with CD34 (*green*), CD11b (*red*), and $CB_2$ receptor (*blue*) antibodies. The $CB_2$ receptor was also present in CD45R/B220$^+$ (*green*) and CD11b$^+$ (*red*) cells. Total cell nuclei were counterstained with Hoechst 33342 (*gray*). The *right column* shows the merged images. *Scale bars*, 50 and 10 $\mu$m in *upper* and *middle panels*, respectively. *B*, transcript levels of the indicated myeloid and microglial markers were analyzed in spinal cord extracts from wild-type mice, either healthy or EAE-induced (clinical score ranging from 2.5 to 3.5). *C*, transcript levels of the indicated elements of the eCB system. Transcript levels were normalized to 18 S RNA expression, referred to healthy mice levels, and provided in arbitrary units (*a.u.*). **, $p < 0.01$ *versus* control.

## RESULTS

*$CB_2$ Cannabinoid Receptor Deficiency Exacerbates EAE Pathogenesis*—Wild-type mice immunized by myelin oligodendrocyte glycoprotein injection developed EAE with the appearance of symptoms starting at day 12.4 ± 4.2 and, after reaching a maximal stage at day 20.2 ± 2.7 (Fig. 1*A*), entered a chronic clinical phase (22, 25) The involvement of the $CB_2$ receptor in the appearance of EAE symptoms was investigated by comparing wild-type and $CB_2^{-/-}$ littermates, which showed that the latter developed a notably higher symptomatic EAE score (Fig. 1, *A* and *B*). The day before sacrifice, magnetic resonance imaging analysis was performed, confirming the existence of an exacerbated neuroinflammatory process in the dorsal spinal cords of $CB_2^{-/-}$ animals as evidenced by the bright signal of low water diffusion areas (Fig. 1*C*). Spinal cord lesions were characterized in further detail by histological analysis. Quantification of neurofilament H immunofluorescence showed an increased axonal loss (Fig. 2*A*) together with extended microglial-cell (CD11b$^+$) activation and T-lymphocyte (CD4$^+$) infiltration in $CB_2$-deficient mice (Fig. 2, *B* and *C*), thus providing further evidence for the exacerbated phenotype of these animals. As $CB_2$ receptors are highly

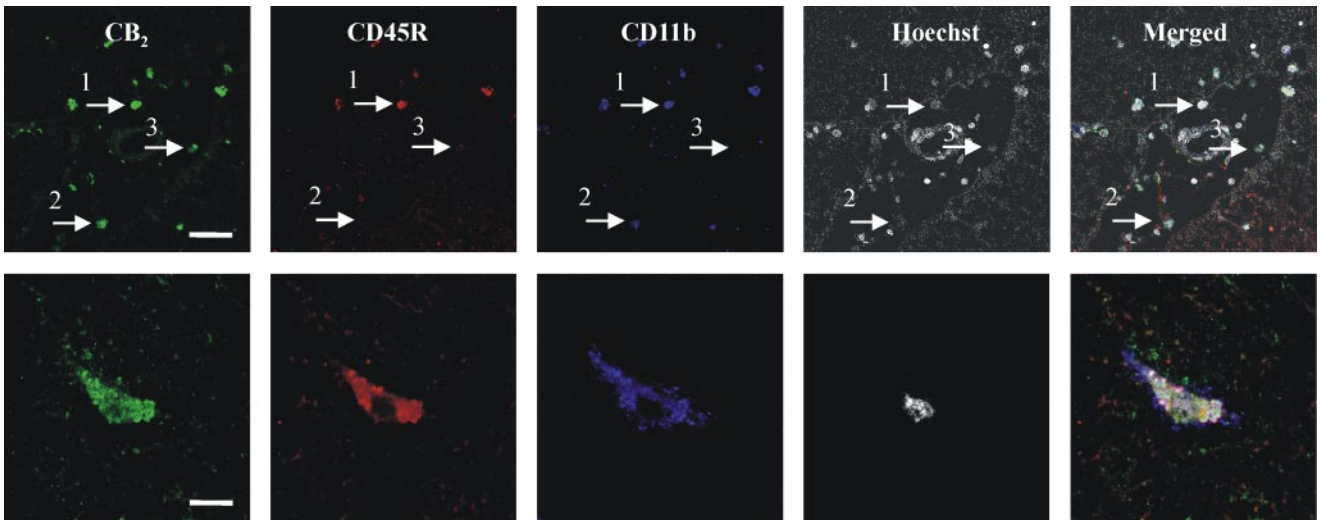


FIGURE 5. **Expression of the $CB_2$ cannabinoid receptor in CD45R$^+$ microglial cells in cortical plaques of multiple sclerosis patients.** Confocal microscopy analyses were performed by using $CB_2$ receptor (*green*), CD45R (*red*), and CD11b (*blue*) antibodies. Images show $CB_2$ receptor expression in CD45$^+$ CD11b$^+$ microglial cells (denoted by *arrows*) (*1*), CD11b$^+$ CD45R$^+$ microglial cells (*2*), and CD11b$^-$CD45R$^+$ cells (*3*) located in the vicinity of blood vessels. Cell nuclei were counterstained with Hoechst 33342 (gray). *Scale bars*, 35 and 10 $\mu$m in *upper* and *lower panels*, respectively.

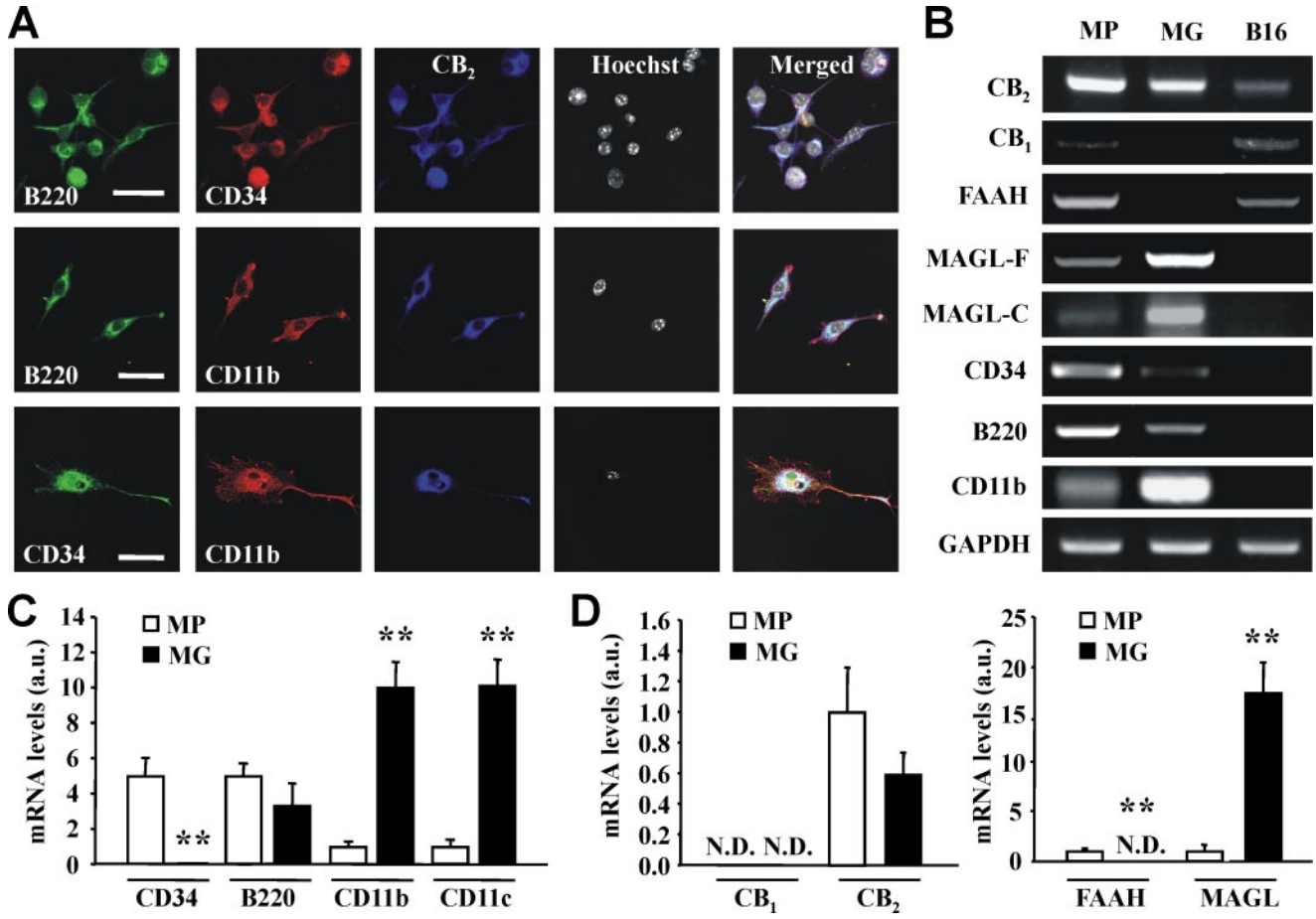


FIGURE 6. **The $CB_2$ cannabinoid receptor is expressed in bone-marrow myeloid progenitors.** *A*, immunofluorescence of cultured myeloid progenitors was performed with the indicated combinations of antibodies against CD34, CD45R/B220, CD11b, and $CB_2$ receptor. Total cell nuclei were counterstained with Hoechst 33342 (*gray*), and the *right column* shows the merged images. *Scale bars*, 25 $\mu$m in *upper* and *middle panels* and 45 $\mu$m in *lower panels*. *B*, reverse transcription-PCR expression analysis of the eCB system receptors ($CB_1$, $CB_2$) and de-activation enzymes FAAH; full-length and catalytic MAGL (*MAGL-F* and *MAGL-C*, respectively) in myeloid progenitors (*MP*), and microglial-like differentiated cells (*MG*). The B16 melanoma cell line was used as a control. *GAPDH*, glyceraldehyde-3-phosphate dehydrogenase. *C*, real-time PCR quantification of the indicated transcripts in myeloid progenitors and microglial-like differentiated cells. *D*, transcript levels of the indicated elements of the eCB system including receptors (*left panel*) and de-activation enzymes (*right panel*). Transcript levels were normalized to 18 S RNA expression and are provided in arbitrary units (*a.u.*). **, $p < 0.01$ *versus* myeloid progenitors; *N.D.*, non-detectable.

expressed in bone marrow immune cells (13, 15), and myeloid progenitor cells can be recruited into the neuroinflamed central nervous system (19–22), we analyzed the presence of cells expressing CD34, a marker for primitive myeloid progenitors. Of interest, an increased number of $CD34^+$ cells was evident in $CB_2$-deficient spinal cords (Fig. 2*D*). Increased proliferation ($Ki\text{-}67^+$ cells) of CD11b and CD34 cell populations was also observed in $CB_2$ knock-out mice (Fig. 2*E*).

*Selective $CB_2$ Cannabinoid Receptor Activation Palliates EAE Symptoms and Pathogenesis*—As $CB_2$ receptor genetic ablation exacerbates EAE pathogenesis, we assessed the impact of $CB_2$ receptor selective activation on disease progression. Daily injections of the $CB_2$-selective agonist HU-308 (29) were performed starting at the day of maximal disease score. In agreement with the observations from $CB_2$-deficient mice, HU-308 treatment improved EAE score and the evolution of the disease when compared with vehicle administration (Fig. 3*A*). The specificity of HU-308 action was confirmed by the use of $CB_2^{-/-}$ mice, in which this agonist was unable to decrease EAE score (data not shown). The analysis of HU-308 administration on tissue histology revealed a strong reduction of spinal cord infiltrates (Fig. 3*B*) that correlated with reduced axonal loss (Fig. 3*C*, *left panel*), microglial activation (Fig. 3*C*, *middle panel*), and myeloid $CD34^+$ cell infiltration (Fig. 3*C*, *right panel*). Of importance, HU-308 administration decreased microglial and infiltrating myeloid cell proliferation (Fig. 3*D*).

*Expression of the eCB System in Myeloid Progenitor Cells*—To confirm whether myeloid progenitors with the ability to generate microglial cells may be directly targeted by $CB_2$ receptor activation, we examined spinal cord sections of EAE mice. Confocal microscopy confirmed the expression of $CB_2$ receptors in $CD34^+$ myeloid progenitor cells (Fig. 4*A*). Importantly, these cells were also positive for CD11b, supporting that recruited cells are prone to microglial differentiation (19–22). In addition, $CB_2$ receptors were expressed in $CD11b^+$ cells that co-express CD45R/B220 (Fig. 4*A*), a marker that has been shown to identify myeloid progenitors with the potential to differentiate to microglial cells (22). Real-time PCR quantification analysis revealed that in EAE mice transcript levels of CD34, CD45R/B220, CD11b, and CD11c were increased in spinal cord extracts (Fig. 4*B*). The eCB system elements were also up-regulated during EAE, and the maximal induction was observed for $CB_2$

receptor expression, which was accompanied by increased expression of the $CB_1$ receptor and the degrading enzymes fatty acid amide hydrolase (FAAH) and monoacylglycerol lipase (MAGL; Fig. 4*C*). Next, we analyzed the expression of $CB_2$ receptors in brain sections of MS patients. $CB_2$ receptors were expressed in microglial cells of plaques located in the vicinity of blood vessels (28), and importantly, a subpopulation of these cells was shown to co-express the myeloid marker CD45RB (Fig. 5).

Finally, we verified the expression of $CB_2$ receptors in myeloid progenitors from bone marrow-derived cultures. Immunofluorescence analysis showed the co-expression of $CB_2$ receptors with CD34 and CD45R/B220 (Fig. 6*A*). $CB_2$ receptors were also present in committed cells that express CD11b together with CD45R/B220 or CD34 (Fig. 6*A*). Gene expression analysis by reverse transcription-PCR (Fig. 6*B*) and quantitative PCR (Fig. 6, *C* and *D*, *left panel*) of myeloid progenitor cell cultures confirmed the expression of *CD34*, *CD45R/B220*, and *CD11b*. Microglial-like cell differentiation reduced the expression of CD34, whereas increased expression of CD11b and CD11c was observed. $CB_2$ receptor transcripts were highly expressed in myeloid progenitors and were also evident in differentiated microglial-like cells (Fig. 6, *B* and *D*). In contrast, $CB_1$ receptor mRNA was hardly detectable in myeloid progenitors and was below detection limits after differentiation. The eCB degrading enzymes showed opposite patterns of expression with decreased FAAH and up-regulated MAGL transcripts upon differentiation (Fig. 6*D*, *right panel*).

*The $CB_2$ Cannabinoid Receptor Controls Bone Marrow-derived Myeloid Cell Trafficking*—The mechanism of $CB_2$ receptor regulation on myeloid cell recruitment and microglial replenishment during EAE pathogenesis was further investigated. Bone marrow cells from EAE mice were obtained at the end of the experiment and analyzed by flow cytometry. The number of $CD11b^+$ cells was not altered in $CB_2^{-/-}$ mice when compared with wild-type mice (Fig. 7*A*, *upper panel*). In contrast, $CD34^+$ cells were increased in mice lacking the $CB_2$ receptor (Fig. 7*A*, *lower panel*), whereas the opposite was observed upon HU-308 administration ($CD34^+$ cells 2.4 ± 0.2 and 1.4 ± 0.3% in vehicle- and HU-308-treated mice, respectively; $p < 0.01$). Flow cytometry (Fig. 7*B*) and real-time PCR quantification analysis (Fig. 7*C*) of PBMCs obtained from the same EAE mice supported that, in parallel with bone marrow cell profiles, $CD34^+$ but not $CD11b^+$ cells were expanded into circulating blood cells in mice lacking the $CB_2$ receptor. These findings are in line with the aforementioned higher number of $CD34^+$ and $CD11b^+$ cells found in spinal cords of $CB_2^{-/-}$ mice, suggesting that the $CB_2$ receptor can control myeloid progenitor cell trafficking toward neuroinflamed tissue.

An analysis of the *in vivo* expression of chemokine ligands and receptors was performed in EAE spinal cord and bone marrow. $CB_2$ receptor ablation up-regulated chemokines and receptors known to be important in microglial recruitment to inflammatory lesions (30). Thus, CCL2, CCL3, and CCL5 transcript levels were increased, and similarly, their principal receptors CCR2 and CCR1 were also induced in bone marrow (Fig. 8, *A* and *B*). On the other hand, HU-308 administration resulted

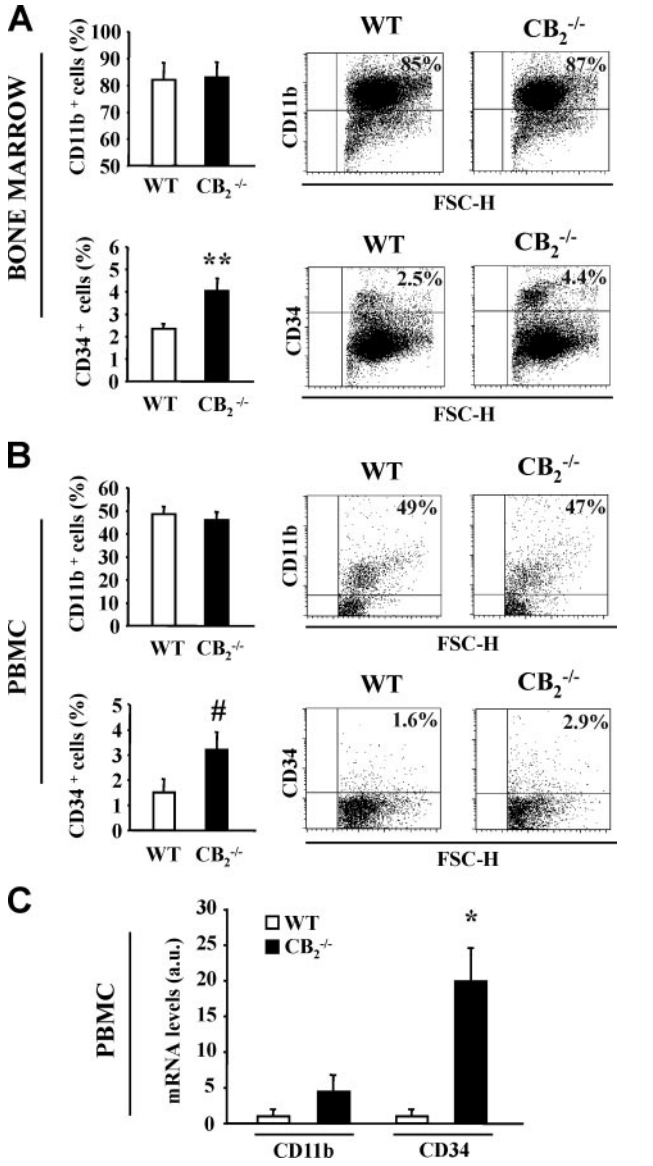


FIGURE 7. **The $CB_2$ cannabinoid receptor regulates myeloid progenitor cell trafficking.** *A*, flow cytometry analysis of $CD11b^+$ and $CD34^+$ cells within bone marrow cells obtained from WT and $CB_2^{-/-}$ EAE mice at the end of the experiment ($n = 8$ each group). Representative histograms are shown (*right panels*). *B*, flow cytometry analysis of $CD11b^+$ and $CD34^+$ cells of PBMCs from WT and $CB_2^{-/-}$ EAE mice. *C*, levels of CD11b and CD34 transcripts were determined by real-time quantitative PCR in PBMC extracts of the same animals. Transcript levels were normalized to 18 S RNA expression, referred to WT levels, and provided in arbitrary units (*a.u.*). #, $p < 0.1$, *, $p < 0.05$, **, $p < 0.01$ *versus* WT.

in an overall reduction of these chemoattractant ligands and receptors (Fig. 8, *C* and *D*).

*Increased Bone Marrow-derived Cell Recruitment in Spinal Cords of $CB_2$ Receptor-deficient EAE Mice*—To confirm the involvement of the $CB_2$ receptor in microglial replenishment from myeloid progenitors, bone marrow GFP-labeled cells derived from healthy EGFP transgenic mice were transferred into EAE-induced wild-type and $CB_2^{-/-}$ mice before symptom appearance (Fig. 9*A*). At the end of the experiment, flow cytometry analysis revealed the presence of a significant population of grafted cells in the PBMC fraction obtained from the blood of recipient animals (9.6 ± 1.1%), of which the majority (96.1 ±

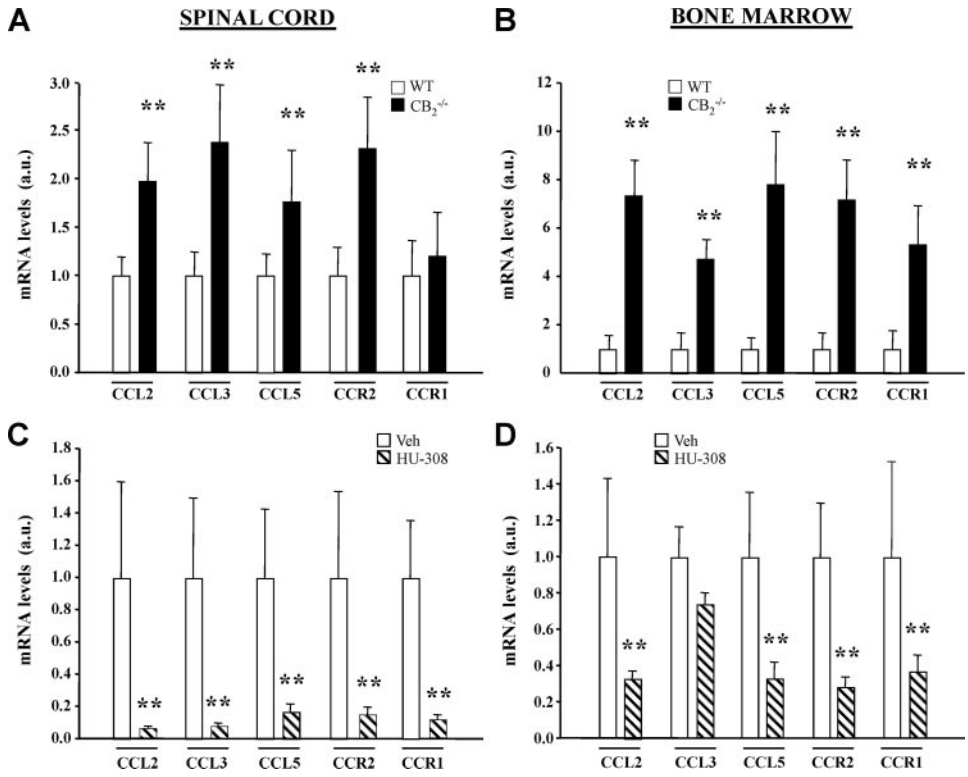


FIGURE 8. **The $CB_2$ cannabinoid receptor regulates the expression of chemokine ligands and receptors.** Real-time PCR analysis of the indicated chemokines and their receptors normalized to 18 S RNA transcript levels in spinal cord (*A*) and bone marrow (*B*) extracts obtained from WT and $CB_2^{-/-}$ EAE mice at the end of the experiment ($n = 8$ each group). *a.u.*, arbitrary units. A similar analysis was performed in spinal cord (*C*) and bone marrow (*D*) of wild-type EAE mice treated with vehicle (*Veh*, *white bars*) or HU-308 (*striped bars*; 15 mg/kg daily; $n = 5$ each group). Results are provided in arbitrary units and referred to wild-type (*A* and *B*) or vehicle-treated mice (*C* and *D*). **, $p < 0.01$ *versus* WT or vehicle-treated mice.

2.7%) co-expressed CD11b (Fig. 9*B*, *upper panel*). $CB_2^{-/-}$ mice showed an increased number of total circulating $CD34^+$ cells, which was also evident within the $GFP^+$ population (Fig. 9*B*, *lower panel*). Spinal cord sections were also analyzed, and bone marrow-derived $GFP^+$ cells were observed (Fig. 9*C*). Quantification of $GFP^+$ cells showed a higher number of infiltrating myeloid cells in $CB_2^{-/-}$ mice than in wild-type littermates (Fig. 9*C*). Further immunofluorescence analysis evidenced that transferred $GFP^+$ cells constituted differentiated microglial infiltrates in the spinal cord as they expressed the CD11b marker (91.2 ± 3.6%), whereas in some $GFP^+$ cells (20.2 ± 3.6%), CD34 expression was still evident (Fig. 9*D*). Moreover, the fraction of $GFP^+CD11b^+$ cells within the total $CD11b^+$ microglial cell pool was elevated in $CB_2^{-/-}$ mice (Fig. 9*E*). In summary, these results support the involvement of $CB_2$ receptors in bone marrow-derived myeloid cell recruitment toward neuroinflamed tissue.

## DISCUSSION

Alterations of the eCB system have been implicated in the pathogenesis of several neurodegenerative disorders, and activation of cannabinoid receptors exerts neuroprotection in various models of brain damage including excitotoxicity, traumatic brain injury, and stroke (1, 31). Moreover, cannabinoid administration elicits an improvement of symptoms of different neuroinflammatory situations including EAE (2, 12). Genetic and pharmacological studies support that neuronal $CB_1$ receptor expression is required for cannabinoid-mediated suppression of EAE symptoms (4, 14, 32). In contrast, other reports have pointed to the involvement of both $CB_1$ and $CB_2$ receptors in the beneficial effects of cannabinoids in MS models (4, 7, 9, 11, 33). Thus, the precise role of $CB_2$ receptors in EAE pathology is still a matter of debate.

Infiltrating T-cells and resident microglia make a major contribution to the ethiopathology of neuroinflammation and neurodegeneration in MS patients, as well as in animal models of the disease (17). In addition, recent research has shown that brain-resident microglia can be replenished by grafted bone marrow-derived myeloid progenitors (19–21, 34). In particular, under neuroinflammatory conditions such as EAE, bone marrow-derived $CD34^+$ myeloid progenitors mobilize through the blood and target the inflamed brain, allowing the recruitment of new microglial cells (22).[8] By using various experimental approaches, here we demonstrate that $CB_2$ receptors play an important role in the control of EAE pathology and provide evidence for the mechanism of $CB_2$ action, namely the targeting of myeloid progenitor cells. Thus, the absence of $CB_2$ receptors significantly exacerbates EAE symptoms and myeloid cell recruitment into the inflamed central nervous system, whereas the opposite is observed upon $CB_2$-selective agonist administration. Control of microglial recruitment by $CB_2$ receptors involves the regulation of important mediators of cell trafficking such as chemokines and their receptors. Genetic and pharmacological models of $CB_2$ receptor manipulation elicit changes in the expression of chemokines that promote myeloid cell recruitment to neuroinflammatory lesions such as CCL2, CCL3, and CCL5. In addition, expression of their receptors CCR2 and CCR1 was also affected. Our results are in line with the role of the CCL2-CCR2 axis in microglial replenishment derived from inflammatory monocytes (35, 36). Likewise, CCR2 is required for bone marrow-derived microglial recruitment and the development of neuropathic pain (37). In this context, stimulation of human monocytes with $CB_2$-selective agonists has been shown to inhibit CCL2- and CCL3-mediated chemotaxis by cross-desensitization of CCR2 and CCR1 (38).

$CB_2$ receptors participate in the control of cell proliferation, survival, and differentiation fate decisions (15). Thus, $CB_2$ receptor activation controls hematopoietic and neural progenitor cell proliferation and differentiation. An inverse relation between $CB_2$ receptor expression and stage of cell differentiation has been

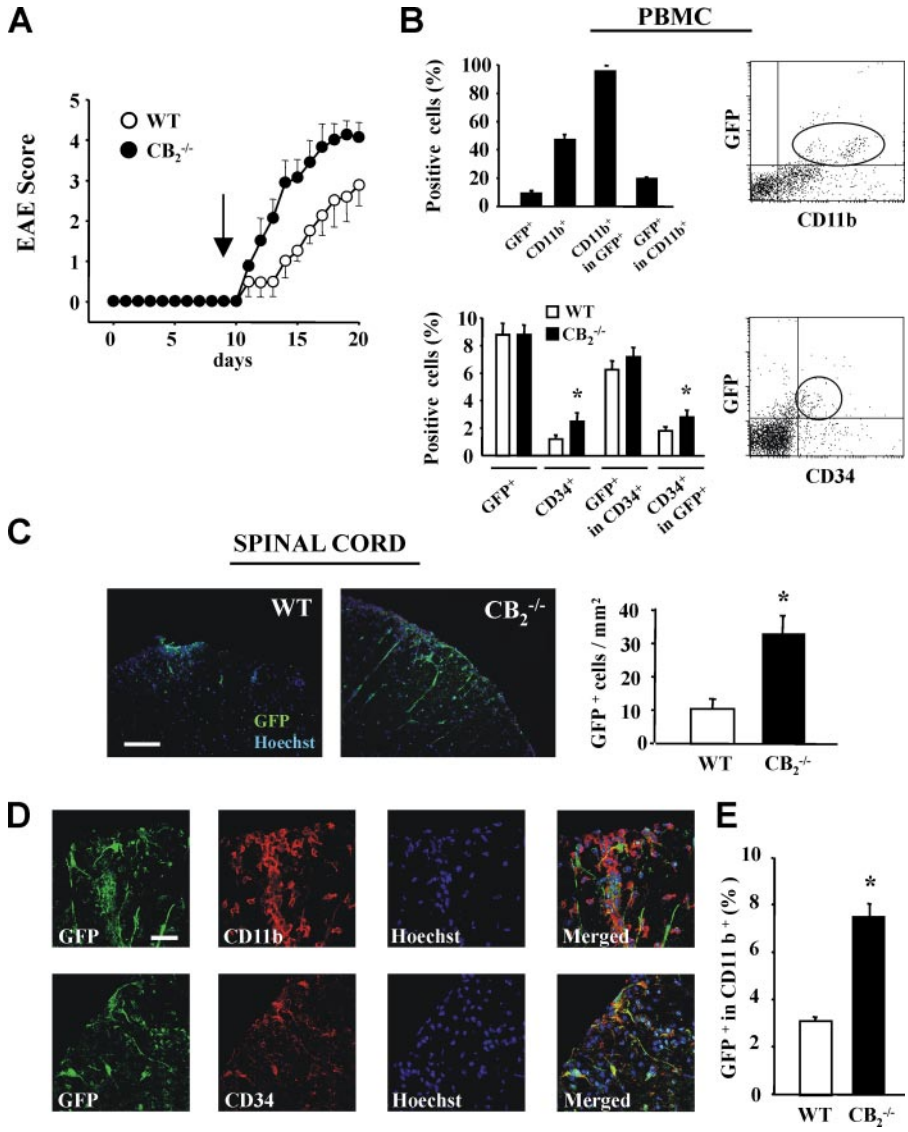


FIGURE 9. **Bone marrow-derived GFP-labeled cell transfer experiments in EAE mice.** *A*, EAE score progression of WT (*open circles*) and $CB_2^{-/-}$ mice (*closed circles*; $n = 6$ each group) subjected to bone marrow GFP-cell injection at day 9 prior to symptom appearance. *B*, at the end of the experiment (day 19), circulating $GFP^+$ bone marrow-derived monocytic cells in the blood of recipient animals were detected by flow cytometry and immunostained with CD11b and CD34 antibodies. *C*, double staining with GFP antibody (*green*) and Hoechst 33342 (*red*) in EAE spinal cord sections (*left panel*). GFP-positive immunoreactive cells were quantified (*right panel*). *D*, high magnification immunofluorescence images obtained with GFP (*green*) and either CD34 or CD11b (*red*) antibodies are shown. Total cell nuclei were counterstained with Hoechst 33342 (*gray*), and the *right column* shows the merged images. *E*, spinal cord-infiltrating $GFP^+CD11b^+$ cells were quantified and referred to the total number of $CD11b^+$ cells. *Scale bars*, 100 and 30 $\mu$m in *C* and *D*, respectively. *, $p < 0.05$ *versus* WT.

shown in neural cells (from neural progenitors to mature neurons and neuroglial cells) (39) and B-cells (from virgin B-cells to centroblasts) (40), and $CB_2$ receptor activation and overexpression has been reported to block neutrophil cell differentiation (41). It is therefore conceivable that changes in cell proliferation, as observed in our study, and differentiation may also contribute to $CB_2$ receptor-regulated myeloid progenitor trafficking.

Our data agree with the current notion that microglial cells express $CB_2$ receptors (42), which are strongly up-regulated in animal models of neuroinflammation (16) and in plaques of MS patients (28, 43). Microglial cells synthesize and degrade eCB ligands such as 2-arachidonoylglycerol (12), the levels of which are negatively controlled by the interferon-$\gamma$ released by primed T-cells invading the central nervous system during EAE, thus indicating that impaired 2-arachidonoylglycerol production may be associated with neurodegeneration in EAE (44). In addition, cannabinoids down-regulate the production of proinflammatory cytokines (mostly interleukin-1$\beta$, interleukin-6, and tumor necrosis factor-$\alpha$ by microglial cells and interleukin-2, interferon-$\gamma$, and granulocyte-macrophage colony-stimulating factor by autoreactive T cells), as well as of nitrogen and oxygen reactive species (6, 12, 13). Overall eCBs via $CB_2$ receptors appear to play a key neuroimmunomodulatory role in EAE not only by preventing T-cell-mediated neurodegeneration (2, 4) but also by inhibiting bone marrow-derived myeloid cell recruitment (present report) and microglial activation (11).

The preclinical studies evidencing the ability of cannabinoids to manage EAE symptoms have fostered the investigation for their potential translation to the clinic (2, 18, 45, 46). Beneficial cannabinoid actions in MS patients, supported by large scale phase III clinical trials, include alleviation of spasticity and tremor, neuropathic pain, and nocturia. Nonetheless, therapies for MS management should be able to prevent not only those symptoms but also neuroinflammation, demyelination, axonal loss, and neurodegeneration to exert a clinically relevant impact in the secondary phase of the disease (2, 17). In this context, cannabinoids constitute a very attractive possibility for therapeutic intervention as they are neuroprotective (31), prevent demyelination (9), and exert a wide array of anti-inflammatory actions (12, 13). The use of selective $CB_2$ receptor agonists for the treatment of MS, and perhaps of other neuroinflammatory conditions, constitutes therefore an attractive possibility owing to the selective role of this cannabinoid receptor type in immune regulation and to the absence of marijuana-like psychoactive effects associated with its activation (15, 23).

*Acknowledgments—We are indebted to our laboratory colleagues for their support and encouragement, to I. del Valle and A. Sánchez for fruitful scientific discussions and collaboration, to A. Egia and E. Resel for technical support, and to M. Fernández and D. Castejón for excellent assistance in MRI imaging.*

## REFERENCES


1. Piomelli, D. (2003) *Nat. Rev. Neurosci.* **4,** 873–884
2. Pryce, G., and Baker, D. (2005) *Trends Neurosci.* **28,** 272–276
3. Cabranes, A., Venderova, K., de Lago, E., Fezza, F., Sanchez, A., Mestre, L., Valenti, M., Garcia-Merino, A., Ramos, J. A., Di Marzo, V., and Fernandez-Ruiz, J. (2005) *Neurobiol. Dis.* **20,** 207–217
4. Maresz, K., Pryce, G., Ponomarev, E. D., Marsicano, G., Croxford, J. L., Shriver, L. P., Ledent, C., Cheng, X., Carrier, E. J., Mann, M. K., Giovannoni, G., Pertwee, R. G., Yamamura, T., Buckley, N. E., Hillard, C. J., Lutz, B., Baker, D., and Dittel, B. N. (2007) *Nat. Med.* **13,** 492–497
5. Baker, D., Pryce, G., Croxford, J. L., Brown, P., Pertwee, R. G., Huffman, J. W., and Layward, L. (2000) *Nature* **404,** 84–87
6. Croxford, J. L., and Miller, S. D. (2003) *J. Clin. Investig.* **111,** 1231–1240
7. Ortega-Gutierrez, S., Molina-Holgado, E., Arevalo-Martin, A., Correa, F., Viso, A., Lopez-Rodriguez, M. L., Di Marzo, V., and Guaza, C. (2005) *FASEB J.* **19,** 1338–1440
8. Molina-Holgado, E., Vela, J. M., Arevalo-Martin, A., Almazan, G., Molina-Holgado, F., Borrell, J., and Guaza, C. (2002) *J. Neurosci.* **22,** 9742–9753
9. Arévalo-Martin, A., Vela, J. M., Molina-Holgado, E., Borrell, J., and Guaza, C. (2003) *J. Neurosci.* **23,** 2511–2516
10. Jackson, S. J., Pryce, G., Diemel, L. T., Cuzner, M. L., and Baker, D. (2005) *Neuroscience* **134,** 261–268
11. Eljaschewitsch, E., Witting, A., Mawrin, C., Lee, T., Schmidt, P. M., Wolf, S., Hoertnagl, H., Raine, C. S., Schneider-Stock, R., Nitsch, R., and Ullrich, O. (2006) *Neuron* **49,** 67–79
12. Walter, L., and Stella, N. (2004) *Br. J. Pharmacol.* **141,** 775–785
13. Klein, T. W. (2005) *Nat. Rev. Immunol.* **5,** 400–411
14. Pryce, G., and Baker, D. (2007) *Br. J. Pharmacol.* **150,** 519–525
15. Fernández-Ruiz, J., Romero, J., Velasco, G., Tolón, R. M., Ramos, J. A., and Guzmán, M. (2007) *Trends Pharmacol. Sci.* **28,** 39–45
16. Maresz, K., Carrier, E. J., Ponomarev, E. D., Hillard, C. J., and Dittel, B. M. (2005) *J. Neurochem.* **95,** 437–445
17. Hauser, S. L., and Oksenberg, J. R. (2006) *Neuron* **52,** 61–76
18. Collin, C., Davies, P., Mutiboko, I. K., and Ratcliffe, S. (2007) *Eur. J. Neurol.* **14,** 290–296
19. Vallieres, L., and Sawchenko, P. E. (2003) *J. Neurosci.* **23,** 5197–5207
20. Simard, A. R., and Rivest, S. (2004) *FASEB J.* **18,** 998–1000
21. Djukic, M., Mildner, A., Schmidt, H., Czesnik, D., Brück, W., Priller, J., Nau, R., and Prinz, M. (2006) *Brain* **29,** 2394–2403
22. Davoust, N., Vuaillat, C., Cavillon, G., Domenget, C., Hatterer, E., Bernard, A., Dumontel, C., Jurdic, P., Malcus, M., Confavreux, C., Belin, M. F., and Nataf, S. (2006) *FASEB J.* **20,** 2081–2092
23. Mackie, K. (2006) *Annu. Rev. Pharmacol. Toxicol.* **46,** 101–122
24. Buckley, N. E., McCoy, K. L., Mezey, E., Bonner, T., Felder, C. C., Glass, M., and Zimmer, A. (2000) *Eur. J. Pharmacol.* **396,** 141–149
25. Nataf, S., Carroll, S. L., Wetsel, R. A., Szalai, A. J., and Barnum, S. R. (2000) *J. Immunol.* **165,** 5867–5873
26. Aguado, T., Palazuelos, J., Monory, K., Stella, N., Cravatt, B., Lutz, B., Marsicano, G., Kokaia, Z., Guzmán, M., and Galve-Roperh, I. (2006) *J. Neurosci.* **26,** 1551–1561
27. Servet-Delprat, C., Arnaud, S., Jurdic, P., Nataf, S., Grassetn, M. F., Soulas, C., Domenget, C., Destaing, O., Rivollier, A., Perret, M., Dumontel, C., Hanau, D., Gilmore, G. L., Belin, M. F., Rabourdin-Combe, C., and Mouchiroud, G. (2002) *BMC Immunol.* **3,** 15
28. Benito, C., Romero, J. P., Tolon, R. M., Clemente, D., Docagne, F., Hillard, C. J., Guaza, C., and Romero, J. (2007) *J. Neurosci.* **27,** 2396–2402
29. Hanus, L., Breuer, A., Tchilibon, S., Shiloah, S., Goldenberg, D., Horowitz, M., Pertwee, R. G., Ross, R. A., Mechoulam, R., and Fride, E. (1999) *Proc. Natl. Acad. Sci. U. S. A.* **96,** 14228–14233
30. Hanisch, U., and Kettenman, H. (2007) *Nat. Neurosci.* **10,** 1387–1394
31. Mechoulam, R., Spatz, M., and Shohami, E. (2002) *Science's STKE* **129,** E5
32. Croxford, J. L., Pryce, G., Jackson, S. J., Ledent, C., Giovannoni, G., Pertwee, R. G., Yamamura, T., and Baker, D. (2007) *J. Neuroimmunol.* **93,** 120–129
33. Docagne, F., Muneton, V., Clemente, D., Ali, C., Loria, F., Correa, F., Hernangomez, M., Mestre, L., Vivien, D., and Guaza, C. (2007) *Mol. Cell. Neurosci.* **34,** 551–561
34. Asheuer, M., Pflumio, F., Benhamida, S., Dubart-Kupperschmitt, A., Fouquet, F., Imai, Y., Aubourg, P., and Cartier, N. (2004) *Proc. Natl. Acad. Sci. U. S. A.* **101,** 3557–3562
35. Mildner, A., Schmidt, H., Nitsche, M., Merkler, D., Hanisch, U. K., Mack, M., Heikenwalder, M., Brück, W., Priller, J., and Prinz, M. (2007) *Nat. Neurosci.* **10,** 1544–1553
36. Babcock, A. A., Kuziel, W. A., Rivest, S., and Owens, T. (2003) *J. Neurosci.* **23,** 7922–7930
37. Zhang, J., Shi, X. Q., Echeverry, S., Mogil, J. S., De Koninck, Y., and Rivest, S. (2007) *J. Neurosci.* **27,** 12396–12406
38. Montecucco, F., Burger, F., Mach, F., and Steffens, S. (2008) *Am. J. Physiol.* **294,** H1145–H1155
39. Palazuelos, J., Aguado, T., Egia, A., Mechoulam, R., Guzmán, M., and Galve-Roperh, I. (2006) *FASEB J.* **20,** 2405–2407
40. Carayon, P., Marchand, J., Dussossoy, D., Derocq, J. M., Jbilo, O., Bord, A., Bouaboula, M., Galiegue, S., Mondiere, P., Penarier, G., Fur, G. L., Defrance, T., and Casellas, P. (1998) *Blood* **92,** 3605–3615
41. Alberich, Jordá, M., Rayman, N., Tas, M., Verbakel, S. E., Battista, N., van Lom, K., Löwenberg, B., Maccarrone, M., and Delwel, R. (2004) *Blood* **104,** 526–534
42. Carrier, E. J., Querrán, C. S., Barkmeier, A. J., Breese, N. M., Yang, W., Nithipatikom, K., Pfister, S. L., and Campbell, W. B. (2004) *Mol. Pharmacol.* **65,** 999–1007
43. Yiangou, Y., Facer, P., Durrenberger, P., Chessell, I. P., Naylor, A., Bountra, C., Banati, R. R., and Anand, P. (2006) *BMC Neurol.* **6,** 12
44. Witting, A., Chen, L., Cudaback, E., Straiker, A., Walter, L., Rickman, B., Moller, T., Brosnan, C., and Stella, N. (2006) *Proc. Natl. Acad. Sci. U. S. A.* **103,** 6362–6367
45. Zajicek, J. P., Sanders, H. P., Wright, D. E., Vickery, P. J., Ingram, W. M., Reilly, S. M., Nunn, A. J., Teare, L. J., Fox, P. J., and Thompson, A. J. (2005) *J. Neurol. Neurosurg. Psychiatry* **76,** 1664–1669
46. Wade, D. T., Makela, P. M., House, H., Bateman, C., and Robson, P. (2006) *Mult. Scler.* **12,** 639–645